



HAL
open science

Liquid Overlay Technique allows the generation of homogeneous osteosarcoma, glioblastoma, lung and prostate adenocarcinoma spheroids that can be used for drug cytotoxicity measurements

Camille Jubelin, Javier Muñoz-Garcia, Denis Cochonneau, Emilie Ollivier, François M Vallette, Marie Françoise Heymann, Lisa Oliver, Dominique Heymann

► To cite this version:

Camille Jubelin, Javier Muñoz-Garcia, Denis Cochonneau, Emilie Ollivier, François M Vallette, et al.. Liquid Overlay Technique allows the generation of homogeneous osteosarcoma, glioblastoma, lung and prostate adenocarcinoma spheroids that can be used for drug cytotoxicity measurements. *Frontiers in Bioengineering and Biotechnology*, In press, 11, pp.1260049. 10.3389/fbioe.2023.1260049 . inserm-04221908

HAL Id: inserm-04221908

<https://inserm.hal.science/inserm-04221908>

Submitted on 28 Sep 2023

HAL is a multi-disciplinary open access archive for the deposit and dissemination of scientific research documents, whether they are published or not. The documents may come from teaching and research institutions in France or abroad, or from public or private research centers.

L'archive ouverte pluridisciplinaire **HAL**, est destinée au dépôt et à la diffusion de documents scientifiques de niveau recherche, publiés ou non, émanant des établissements d'enseignement et de recherche français ou étrangers, des laboratoires publics ou privés.

1 **Technical Report: Liquid Overlay Technique allows the generation of homogeneous**
2 **osteosarcoma, glioblastoma, lung and prostate adenocarcinoma spheroids that can be**
3 **used for drug cytotoxicity measurements**

4
5 Camille Jubelin^{1,2,3}, Javier Muñoz-Garcia^{1,2}, Denis Cochonneau², Emilie Ollivier²,
6 François Vallette^{2,4}, Marie-Françoise Heymann^{1,2}, Lisa Oliver^{4,5}, Dominique Heymann^{1,2,6,#}

7
8 ¹ Nantes Université, CNRS, US2B, UMR 6286, 44000, Nantes, France

9 ² Institut de Cancérologie de l'Ouest, Tumor Heterogeneity and Precision Medicine Lab.,
10 44805, Saint-Herblain, France

11 ³ Atlantic Bone Screen, 44800 Saint-Herblain, France

12 ⁴ Nantes Université, INSERM, CRCI²NA, UMR1307, 44000, Nantes, France

13 ⁵ CHU de Nantes, Nantes, France

14 ⁶ Department of Oncology and Metabolism, Medical School, University of Sheffield,
15 Sheffield, UK

16
17 **Running title:** Technical Report: Homogeneous generation of tumor spheroids

18
19 **#Corresponding authors**

20 Prof. D. Heymann, Institut de Cancérologie de l'Ouest, Blvd Jacques Monod, 44805 Saint-
21 Herblain, France

22 Email: dominique.heyman@univ-nantes.fr

23
24
25

26 **ABSTRACT**

27 **Introduction:** The mechanisms involved in cancer initiation, progression, drug resistance,
28 and disease recurrence are traditionally investigated through *in vitro* adherent monolayer (2D)
29 cell models. However, solid malignant tumor growth is characterized by progression in three
30 dimensions (3D), and an increasing amount of evidence suggests that 3D culture models, such
31 as spheroids, are suitable for mimicking cancer development. The aim of this report was to
32 reaffirm the relevance of simpler 3D culture methods to produce highly reproducible
33 spheroids, especially in the context of drug cytotoxicity measurements.

34 **Methods:** Human A549 lung adenocarcinoma, LnCaP prostate adenocarcinoma,
35 MNNG/HOS osteosarcoma and U251 glioblastoma cell lines were grown into spheroids for
36 20 days using either Liquid Overlay Technique (LOT) or Hanging Drop (HD) in various
37 culture plates. Their morphology was examined by microscopy. Sensitivity to doxorubicin
38 was compared between MNNG/HOS cells grown in 2D and 3D.

39 **Results:** For all cell lines studied, the morphology of spheroids generated in round-bottom
40 multiwell plates was more repeatable than that of those generated in flat-bottom multiwell
41 plates. HD had no significant advantage over LOT when the spheroids were cultured in
42 round-bottom plates. Finally, the IC₅₀ of doxorubicin on MNNG/HOS cultured in 3D was
43 18.8 times higher than in 2D cultures (3D IC₅₀ = 15.07 ± 0.3 μM; 2D IC₅₀ = 0.8 ± 0.4 μM;
44 *p<0.05).

45 **Discussion:** In conclusion, we propose that the LOT method, despite and because of its
46 simplicity, is a relevant 3D model for drug response measurements that could be scaled up for
47 high throughput screening.

48

49 INTRODUCTION

50

51 For several years, there has been increasing evidence of the usefulness of three-dimensional
52 (3D) cultures for the study of solid tumors compared to conventional monolayer (2D)
53 cultures. Indeed, differences in transcriptome, proteome, drug response, etc. have been
54 described for several cancer types using different 3D culture methods (Imamura et al., 2015;
55 Bingel et al., 2017; Elia et al., 2017; Wisdom et al., 2018; Thippabhotla et al., 2019). In many
56 cases, these 3D cultures better represent *in vivo* tumors than their 2D counterparts (Weeber et
57 al., 2015; Ganesh et al., 2019), making them more suitable for the description of tumor
58 behavior.

59 Spheroids are one of the most commonly used 3D cell models due to their simplicity. They
60 consist of the aggregation of cells to form a multicellular mass. This spherical organization
61 gives cancer cells properties not observed in 2D, such as the generation of a transport gradient
62 or a stratified structure. Spheroids can be generated using several 3D culture methods (Jubelin
63 et al., 2022), including liquid and scaffold-based methods. Although the first method is rather
64 simple, it may not allow the generation of spheroids (Figure 1). On the other hand, scaffold-
65 based methods may generate spheroids, but they may be dispersed in the matrix, which would
66 increase the time needed to analyze them properly (Imamura et al., 2015). This, in turn, may
67 limit their use in a high-throughput setting.

68 The production of reproducible spheroids is of particular importance in the context of drug
69 screening. While repeatability is easily achieved in 2D, where all cells are exposed to the
70 same amount of compounds, the transport gradient inherent in 3D culture implies that cells
71 localized to the core of the spheroids may be less exposed to the drug than those on the outer
72 layer. Ensuring that homogeneous spheroids are generated is therefore particularly important,

73 as spheroid morphology can play an important role in treatment response. However, this is
74 often overlooked in studies comparing drug response between 2D and 3D cultures.
75 State-of-the-art 3D culture methods using bioprinting or microfluidics have been described
76 (Miller et al., 2018; Pinho et al., 2021), but they require very specific equipment, complicate
77 the analysis process and can be difficult to scale up. Therefore, the aim of the present report
78 was to reaffirm the relevance of simpler 3D culture methods to produce highly reproducible
79 spheroids, especially in the context of drug treatment. Two liquid-based cultures were
80 investigated: Liquid Overlay Technique (LOT), which uses culture vessels treated to prevent
81 cells from adhering to their surface, and Hanging Drop (HD), which uses gravity to aggregate
82 cells. Both methods are widely used and therefore well documented. Using LOT and round-
83 bottomed multi-well plates, highly reproducible spheroids of A549 lung adenocarcinoma,
84 LnCaP adenocarcinoma, MNNG/HOS osteosarcoma and U251 glioblastoma cell lines were
85 generated. This method had the advantage of allowing rapid aggregation of cells into
86 spheroids with repeatable morphologies, being inexpensive and implementable in any
87 laboratories. The morphological parameters of the spheroids were easy to assess using
88 microscopic approaches, since the rounded bottom allowed the spheroid to be centered in the
89 well. Finally, this culture model was adapted to drug treatment. But the assessment of the
90 cytotoxicity of the doxorubicin in the 3D specimen required careful selection of the assays.
91 We propose that the LOT method, despite and because of its simplicity, is a relevant 3D
92 model for drug response measurements that could be scaled up for high-throughput screening.

93

94

95 MATERIAL AND METHODS

96

97 *1. Cancer cell lines and culture media*

98 The A549 (CCL-185, ATCC) lung adenocarcinoma cell line, the LnCaP (89110211, ECACC,
99 Saliisbury, UK) prostate adenocarcinoma cell line, the MNNG/HOS (CRL-1547, ATCC, LGC
100 Molsheim, France) osteosarcoma cell line and the U251 (09063001, Sigma-Aldrich, Saint
101 Quentin Fallavier, France) glioblastoma cell line were cultured at 37°C, 5% CO₂ and in an
102 environment saturated in humidity. The A549 were cultured in Ham's F12-K (21127-022,
103 Gibco) complemented with 10% FBS and 2 mM L-Glutamine. The LnCaP were cultured in
104 RPMI complemented (L0501-500, Dutscher) with 10% FBS, 2 mM L-Glutamine and 1 mM
105 sodium pyruvate. The MNNG/HOS were cultured in DMEM 4.5 g/L D-glucose and 0.11 g/L
106 sodium pyruvate (L0106-500, Dutscher, Bernolsheim, France) supplemented with 5% fetal
107 bovine serum (FBS) (CVFSVF00-01, Eurobio Scientific, Les Ulis, France) and 2 mM L-
108 Glutamine (25030-024, Gibco, Paris, France). The U251 were cultured in DMEM 4.5 g/L D-
109 glucose and 0.11 g/L sodium pyruvate complemented with 10% FBS and 2 mM L-Glutamine.
110 All cell lines were regularly tested for the absence mycoplasma.

111

112 **2. 2D cell cultures**

113 Cell lines were maintained as adherent monolayers in T25 or T75 flasks. When the cells
114 reached 90% of confluency, they were passed following classic cell maintenance protocols.
115 To compare sensitivity to drug treatment, the MNNG/HOS cells were cultured in flat-bottom
116 96-well adherent plates (3599, Corning Costar, Boulogne-Billancourt, France).

117

118 **3. 3D cell cultures**

119 In 3D, spheroids were generated in low-adherence flat- (3474, Corning Costar) or round-
120 bottom 96-multiwell plates (174926, Thermo Scientific, Saint-Herblain, France), or round-
121 bottom 384-multiwell plates (4116, Corning Costar) using either the Liquid Overlay
122 Technique (LOT) or the Hanging Drop (HD) method. For cultures using LOT, cells were

123 seeded into low-adherence multiwell plates at a concentration of 20 000 cells per 100 μL or
124 per 50 μL for the 96- and 384-well plates respectively. After 24 hours of culture, 50 μL or 25
125 μL of complete media were added to the wells in the 96- or 384-well plates respectively.
126 Culture media were changed every 2-3 days by replacing 2/3 of the initial volume.
127 For the cultures using HD, cells were suspended at a concentration of 1×10^6 cells/mL. A
128 methylcellulose (HSC001, R&D System, Abington, UK) solution diluted extemporaneously
129 (1/2) with complete culture media was then added to the cell suspension to obtain a ratio of
130 1:4 methylcellulose:suspension (final concentration of methylcellulose: 0.1X). 25 μL droplets
131 of the new suspension were put on the inside of a Petri dish cover. PBS was added to the Petri
132 dish to avoid dehydration of the droplets and the cover was returned to its normal position on
133 the Petri dish. Droplets were incubated in this inversed position for 24h at 37°C , before being
134 transferred to low-adherence multi-well plates, with one droplet/spheroid per well. Culture
135 medium was added to reach a volume identical to the one for the spheroids generated with
136 LOT.

137

138 ***4. Cell viability assay***

139 MNNG/HOS cells were treated with increased concentrations of doxorubicin (0.001 μM , 0.01
140 μM , 0.1 μM , 1 μM , 10 μM and 100 μM). Cell treatment started one day after seeding in either
141 a flat-bottom adherent 96-well plate for 2D culture or a low-adherence round-bottom 96-well
142 plate for 3D culture. After 72h of incubation with doxorubicin, 5 μL of the supernatant was
143 taken from each well. This supernatant was diluted 1/20 in PBS, and 10 μL of this solution
144 was added to 15 μL of LDH Storage buffer and 25 μL Enzyme Mix from the LDH-GloTM
145 Cytotoxicity Assay kit (J2380, Promega, Charbonnières-les-Bains, France). Each sample was
146 put in the well of an opaque white 96-well plate. The plate was left at room temperature for 1

147 hour in the dark. Afterward, luminescence rates were assessed using the VICTOR Nivo
148 (Perkin Elmer, Villebon sur Yevette, France) plate reader.

149 After recovering the samples for the LDH assay, the rest of the supernatant from the treated
150 cells was removed, and the spheroids or cell monolayer were washed and 25 μ L of complete
151 medium was added to each well. Then, fluorescent red and green probes from the
152 LIVE/DEADTM Cell Imaging Kit (InvitrogenTM, Whaltam, MA, USA, ref#R37601) were
153 mixed together and 25 μ L of this suspension were added to each well. After 15 minutes of
154 incubation at room temperature in the dark, cells were imaged by fluorescent microscopy using
155 an Operetta CLS High-Content Analysis System (Perkin Elmer).

156

157 ***5. Microscopic measurement of spheroid morphology***

158 For this study, a spheroid with a satisfactory morphology had to satisfy the following criteria:

159 i) a minimum diameter greater than or equal to 500 μ m, ii) a roundness greater than 0.8, ii)
160 and the presence of a single spheroid per well. Since the diffusion limit of oxygen is 150-200
161 μ m (Olive et al., 1992; Grimes et al., 2014), growing spheroids with a diameter greater than
162 or equal to 500 μ m would ensure the generation of a stratified spheroid with a hypoxic core.

163 A geometric shape that can be easily compared between samples is that of the sphere. In
164 addition, a compound would theoretically diffuse more uniformly in a sphere than in any
165 other type of shape. Therefore, a high roundness is an important morphological parameter that
166 the spheroids must have. Roundness is calculated as $4 \cdot \text{area} / (\pi \cdot \text{major axis}^2)$ and a value of 1
167 corresponds to a perfect disk. Thus, a spheroid with a value of at least 0.8 would closely
168 resemble a sphere. Finally, having of a unique spheroid per well would facilitate the analysis.

169 The free image analysis software FIJI was used for the measurement of the different
170 parameters. After setting the scale, the parameters 'Area', 'Shape descriptors', 'Fit Ellipse'
171 and 'Feret's Diameter' were selected in the 'Analyze Particles' dialog box. After the

172 measurement, the values obtained under the labels 'Area', 'MinFeret' and 'Round' were used
173 to obtain the area of the section, the minimum diameter, and the roundness, respectively. The
174 number of spheroids per well was counted manually.

175

176 *6. Statistical analysis*

177 Statistical analyses were performed using GraphPad Prism 7.0 software (GraphPad Software,
178 La Jolla, CA, USA). Significance was determined using a multiple T test, or a two-way
179 ANOVA test. Error bars show mean \pm standard error of the mean. A p-value \leq 0.05 was
180 considered statistically significant.

181

182 **RESULTS**

183

184 Four cell lines were selected to determine the best 3D culture method for generating
185 spheroids: two cell lines from rare cancers (MNNG/HOS osteosarcoma and U251 glioma
186 cells) and two cell lines from more common cancers (A549 lung adenocarcinoma and LnCaP
187 prostate cancer cells). These cell lines were cultured in 3D using LOT in 96-multiwell plates
188 with flat- or round-bottomed wells for a duration of 20 days. The quality of the spheroids
189 produced was assessed based on their morphological parameters (e.g. area of the spheroid
190 section, minimum diameter, roundness of the sphere, and number of spheroids per well).

191 For all cell lines, except MNNG/HOS at day 20 (*p-value < 0.05), the plate type did not have
192 a statistically significant effect on the area of the section (**Figure 2**). The minimum diameter
193 was significantly increased (*p-value < 0.05) for earlier time points of A549, MNNG/HOS
194 and U251 spheroids grown in round-bottom plates compared to flat-bottom plates spheroids
195 (Figure 2A, C-D). Overall, the spheroids grown in round-bottom plates were slightly larger
196 than those grown in flat-bottom plates and had a minimum diameter of 500 μ m at all time

197 points of the experiment. For the four cell lines, round-bottom plates allowed a faster
198 formation of significantly rounder spheroids compared to those produced in flat-bottom plates
199 (*p-value < 0.05). Finally, only the round-bottom plates ensured the production of a single
200 spheroid per well from day 1 after the seeding and for the entire duration of the experiment.
201 Taken together, these data showed that the A549, LnCaP, MNNG/HOS and U251 cell lines
202 produced spheroids with highly reproducible morphology when grown by LOT in 96-well
203 round-bottom plates.

204

205 Doubling cell density by using well with a smaller diameter did not further improve the
206 morphological parameters of the four cell lines spheroids when assessed 10 days after
207 seeding. Generally, it even tended to increase heterogeneity between replicates as shown by
208 the higher standard deviation (SD) for the spheroids grown into 384-well round-bottom plates
209 (**Figure 3**). In all culture vessels assessed, the HD 3D culture method made it possible to
210 generate a single spheroid per well whose morphology validated size and roundness criteria
211 (diameter > 500 μm , roundness > 0.8) from the first day of culture. However, no significant
212 difference regarding the morphology of the spheroids produced was observed between the
213 spheroids cultured with HD or LOT in round-bottom 96-well plates for all cell lines studied
214 (**Figure 3**).

215

216 To demonstrate the relevance and the efficiency of the LOT in round-bottom plates to
217 evaluate drug response, homogeneous MNNG/HOS spheroids were treated with doxorubicin,
218 and their drug sensitivity was compared to samples grown in 2D. The comparison of cell
219 viability between cells cultured in 2D and in 3D is impaired by the fact that these types of
220 culture lead to highly different cell morphologies and spatial organization. Thus, it is almost
221 impossible to draw definitive conclusions with a sole viability assay, especially if it is an

222 assay originally developed for 2D cultures. In this context, two complementary *in vitro* assays
223 were selected to assess cell viability and response to treatment. MNNG/HOS cells were
224 cultured in 2D or 3D using LOT 96-well plates. Osteosarcoma cells were treated with
225 multiple concentrations of doxorubicin for 72 h. We assessed cell viability based on the
226 culture condition by microscopic observation after LIVE/DEADTM labelling or by measuring
227 the luminescence rate linked to LDH release from dead cells.

228 While the LIVE/DEADTM assay is very useful to assess cell viability in 2D, it lacks resolution
229 in a 3D setting if the imaged specimens are too thick. However, here it allowed to reveal
230 changes in the shape of the cells depending on the concentration of doxorubicin used (**Figure**
231 **4A**). Both in 2D and 3D, we observed an increase in cell size from the concentration 0.01 μM .
232 In 3D, the cells started to shrink again at 1 μM , and this coincided with a decrease in the
233 spheroid diameter. 100 μM of doxorubicin resulted in the disintegration of the spheroids
234 (**Figure 4A**).

235 Although these microscopic observations provide simple and straightforward insights, they
236 are not conclusive in the case of 3D culture. Therefore, an additional assay was added to
237 allow for an unbiased comparison between 2D and 3D. The LDH release assay was performed
238 on the supernatant of the cells previously imaged (**Figure 4B**). The dose-response curves of
239 doxorubicin were different in 2D compared to 3D cell cultures. For the concentrations of 1
240 μM and 5 μM , a significant decrease in cytotoxicity was observed for the 3D culture
241 condition. This translated into an increased IC_{50} in 3D ($3\text{D } \text{IC}_{50} = 15.07 \pm 0.3 \mu\text{M}$), which was
242 18.8 times higher than the IC_{50} in 2D cell cultures ($2\text{D } \text{IC}_{50} = 0.8 \pm 0.4 \mu\text{M}$) (Figure 4,
243 $*p < 0.05$). Overall, the present data showed decreased sensitivity of MNNG/HOS cells to
244 doxorubicin when cultured in 3D rather than in 2D.

245

246 DISCUSSION

247 The ability to form spheroids is not uniform among cell lines, as shown in Figure 1. When
248 grown by the LOT method, the formation of spheroids depends on the intrinsic ability of the
249 cells to aggregate. Modifying the media and/or adding matrix could improve spheroid
250 aggregation. For example, when attempting to grow PC3 cells in 3D using the same medium
251 as in 2D, we did not observe spheroid formation in our LOT condition (**Figure 1**). However,
252 other studies were able to produce round PC3 spheroids with a defined border by growing
253 them with MatrigelTM (Härmä et al., 2010). In addition, several 3D culture media formulations
254 have been described for various application (Fleurence et al., 2016; Gheytañchi et al., 2021).
255 In the context of comparing drug sensitivity between 2D and 3D cultures, it was essential to
256 reduce variations in the parameters tested. The decision was made to grow each cell type in
257 3D with the corresponding medium traditionally used in 2D. This would also enable any
258 laboratory to transition to 3D culture using the same medium they already use for their
259 monolayer cultures. As a results, the primary focus was on modifying the 3D culture method
260 to enhance spheroid generation.

261 The spatial organization of spheroids has a direct impact on both molecular diffusion and cell
262 imaging. It is essential that the spheroids have a homogeneous morphology if we want the
263 observed results to be significant. Most biochemical assays commonly used in research have
264 been originally designed and optimized for 2D cell cultures. Adapting these assays to 3D
265 culture models often requires protocol optimization, as the spatial organization of the
266 spheroids plays a direct role in the diffusion of molecules. By ensuring the generation of
267 spheroids w size aith a consistent size and shape, it is possible to reduce the influence of
268 morphological variability on the significance of the results obtained.

269 Spheroid morphology was assessed by measuring several shape parameters: area of the cross-
270 section and minimum diameter to translate spheroid size, roundness to describe the spheroid
271 shape, and number of spheroids per well. Three main validation criteria for the 3D culture

272 method were selected in this study: i) the spheroids had to have a diameter greater than or
273 equal to 500 μm in order to generate a hypoxic core; ii) the spheroids had to have a shape
274 similar to that of a sphere to ensure that the diffusion of the molecules inside the spheroid was
275 homogeneous between conditions; iii) the 3D culture methods had to generate a single
276 spheroid per well. The 3D culture method that allowed the formation of spheroids meeting all
277 these criteria was LOT in round-bottom 96-well plates for all four cell lines studied (lung
278 adenocarcinoma A549, prostate adenocarcinoma LnCaP, osteosarcoma MNNG/HOS,
279 glioblastoma U251). In addition, the round-bottom plate facilitated image acquisition as the
280 spheroid was always in the center of the well due to gravity. The formation of
281 morphologically homogeneous spheroids across wells appeared to be dependent on the
282 aggregation rate. The round-bottom plates allowed the generation of highly repeatable
283 spheroids by increasing cell-cell contacts.

284 The aim of this study was to provide a simple 3D culture method of the A549, LnCaP,
285 MNNG/HOS and U251 cell lines, for further characterization and use of the spheroids
286 generated to study mechanisms involved in cancer initiation, progression and treatment
287 response. As a proof of concept, the response of MNNG/HOS grown in 3D with LOT in low-
288 adherence 96-well plates to the conventional chemotherapy doxorubicin was measured and
289 compared to 2D culture. The study of drug efficacy in 3D is different from that in 2D. In fact,
290 the spatial organization of the spheroid limits the type of assay that can be used. Indeed, most
291 fluorescent cytotoxic assays on living spheroids would be compromised by the thickness of
292 the sample. A more suitable live assay would require the use of spheroid supernatant, such as
293 the LDH release assay. Alternatively, fixation and clarification or sectioning of the spheroids
294 would be required to image the inside of the sample.

295 Similar to what has already been observed in studies covering other cell lines (Imamura et al.,
296 2015), we describe a decrease in the drug sensitivity of MNNG/HOS cells cultured in 3D

297 compared to 2D. This difference in sensitivity may have multiple explanations. The presence
298 of a diffusion gradient, hypoxic conditions and increased cell-to-cell and cell-to-extracellular
299 matrix (ECM) interactions are all molecular cues that can affect the activation of the signaling
300 pathways, biological processes, and gene and protein expressions involved in drug resistance
301 (Zschenker et al., 2012; Gangadhara et al., 2016; Nath and Devi, 2016; Bingel et al., 2017).

302 The spatial organization of spheroids can also limit treatment efficacy. The presence of a
303 diffusion gradient applies not only to oxygen, but also affects the distribution of
304 chemotherapy molecules. In contrast to 2D cultures, where the doxorubicin is evenly
305 distributed among all cells, the drug may have difficulty reaching the more central cells of the
306 spheroids (Ong et al., 2010; Ma et al., 2012). Usually, larger and more compact spheroids
307 tend to be less treatment-sensitive (Däster et al., 2016; Gencoglu et al., 2018; Thakuri et al.,
308 2019). In the present study, we treated “young” spheroids. We made this choice to minimize
309 the difference in cell number between 2D and 3D cultures, since cell proliferation typically
310 slow down significantly in 3D. It is therefore possible that treating older spheroids could
311 result in an even greater loss of sensitivity than that observed here, as the spheroids would
312 have had more time to compact and establish cellular interactions with their neighboring cells.

313 Hypoxia, which can occur in large spheroids, may also be associated with decreased drug
314 sensitivity. Hypoxia could lead to greater cancer resistance to treatment by promoting the
315 expression of an efflux pump on the cell surface, thereby inducing an anti-apoptotic effect, by
316 promoting genomic instability and slowing cell proliferation (Rohwer and Cramer, 2011).

317 Finally, numerous chemotherapeutic molecules, such as doxorubicin, target cancer cells with
318 a fast proliferation rate. As a result, drugs targeting fast-proliferating cancer cells may prove
319 ineffective against the slowed or arrested proliferation observed in spheroids. (Imamura et al.,
320 2015).

321 In conclusion, we show here that the culture of spheroids in round-bottom multiwell plates
322 using LOT allowed the production of repeatable spheroids for multiple cell lines. This culture
323 method has the advantage of being easy to implement by any laboratory. It is also inexpensive
324 and can be scaled up for high-throughput screening. Although spheroid cultures require
325 optimization of the analysis methods developed for 2D cultures, we were able to show that the
326 efficacy of a treatment can be measured by multiple assays. For all these reasons, the LOT
327 method is a relevant 3D model and we recommend its implementation for any drug screening
328 study.

329

330 **Acknowledgments:** The present works were funded by ANRT (convention CIFRE
331 N°2019/1111). Atlantic Bone Screen paid the salary of Camille Jubelin.

332

333

334 **REFERENCES**

- 335 Bingel, C., Koeneke, E., Ridinger, J., Bittmann, A., Sill, M., Peterziel, H., et al. (2017).
336 Three-dimensional tumor cell growth stimulates autophagic flux and recapitulates
337 chemotherapy resistance. *Cell Death Dis* 8, e3013. doi: 10.1038/cddis.2017.398.
- 338 Däster, S., Amatruda, N., Calabrese, D., Ivanek, R., Turrini, E., Droeser, R. A., et al. (2016).
339 Induction of hypoxia and necrosis in multicellular tumor spheroids is associated with
340 resistance to chemotherapy treatment. *Oncotarget* 8, 1725–1736. doi:
341 10.18632/oncotarget.13857.
- 342 Elia, I., Broekaert, D., Christen, S., Boon, R., Radaelli, E., Orth, M. F., et al. (2017). Proline
343 metabolism supports metastasis formation and could be inhibited to selectively target
344 metastasizing cancer cells. *Nat Commun* 8, 15267. doi: 10.1038/ncomms15267.
- 345 Fleurence, J., Cochonneau, D., Fougerey, S., Oliver, L., Geraldo, F., Terme, M., et al. (2016).
346 Targeting and killing glioblastoma with monoclonal antibody to O-acetyl GD2
347 ganglioside. *Oncotarget* 7, 41172–41185. doi: 10.18632/oncotarget.9226.
- 348 Ganesh, K., Wu, C., O'Rourke, K. P., Szeglin, B. C., Zheng, Y., Sauvé, C.-E. G., et al.
349 (2019). A rectal cancer organoid platform to study individual responses to
350 chemoradiation. *Nat Med* 25, 1607–1614. doi: 10.1038/s41591-019-0584-2.
- 351 Gangadhara, S., Smith, C., Barrett-Lee, P., and Hiscox, S. (2016). 3D culture of Her2+ breast
352 cancer cells promotes AKT to MAPK switching and a loss of therapeutic response.
353 *BMC Cancer* 16, 345. doi: 10.1186/s12885-016-2377-z.
- 354 Gencoglu, M. F., Barney, L. E., Hall, C. L., Brooks, E. A., Schwartz, A. D., Corbett, D. C., et
355 al. (2018). Comparative Study of Multicellular Tumor Spheroid Formation Methods
356 and Implications for Drug Screening. *ACS Biomater. Sci. Eng.* 4, 410–420. doi:
357 10.1021/acsbiomaterials.7b00069.
- 358 Gheyntanchi, E., Naseri, M., Karimi-Busheri, F., Atyabi, F., Mirsharif, E. S., Bozorgmehr, M.,
359 et al. (2021). Morphological and molecular characteristics of spheroid formation in
360 HT-29 and Caco-2 colorectal cancer cell lines. *Cancer Cell International* 21, 204. doi:
361 10.1186/s12935-021-01898-9.
- 362 Grimes, D. R., Kelly, C., Bloch, K., and Partridge, M. (2014). A method for estimating the
363 oxygen consumption rate in multicellular tumour spheroids. *J R Soc Interface* 11,
364 20131124. doi: 10.1098/rsif.2013.1124.
- 365 Härmä, V., Virtanen, J., Mäkelä, R., Happonen, A., Mpindi, J.-P., Knuutila, M., et al. (2010).
366 A Comprehensive Panel of Three-Dimensional Models for Studies of Prostate Cancer
367 Growth, Invasion and Drug Responses. *PLOS ONE* 5, e10431. doi:
368 10.1371/journal.pone.0010431.
- 369 Imamura, Y., Mukohara, T., Shimono, Y., Funakoshi, Y., Chayahara, N., Toyoda, M., et al.
370 (2015). Comparison of 2D- and 3D-culture models as drug-testing platforms in breast
371 cancer. *Oncol Rep* 33, 1837–1843. doi: 10.3892/or.2015.3767.

- 372 Jubelin, C., Muñoz-Garcia, J., Griscom, L., Cochonneau, D., Ollivier, E., Heymann, M.-F., et
373 al. (2022). Three-dimensional in vitro culture models in oncology research. *Cell &*
374 *Bioscience* 12, 155. doi: 10.1186/s13578-022-00887-3.
- 375 Ma, H., Jiang, Q., Han, S., Wu, Y., Cui Tomshine, J., Wang, D., et al. (2012). Multicellular
376 tumor spheroids as an in vivo-like tumor model for three-dimensional imaging of
377 chemotherapeutic and nano material cellular penetration. *Mol Imaging* 11, 487–498.
- 378 Miller, C. P., Tsuchida, C., Zheng, Y., Himmelfarb, J., and Akilesh, S. (2018). A 3D Human
379 Renal Cell Carcinoma-on-a-Chip for the Study of Tumor Angiogenesis. *Neoplasia* 20,
380 610–620. doi: 10.1016/j.neo.2018.02.011.
- 381 Nath, S., and Devi, G. R. (2016). Three-Dimensional Culture Systems in Cancer Research:
382 Focus on Tumor Spheroid Model. *Pharmacol Ther* 163, 94–108. doi:
383 10.1016/j.pharmthera.2016.03.013.
- 384 Olive, P. L., Vikse, C., and Trotter, M. J. (1992). Measurement of oxygen diffusion distance
385 in tumor cubes using a fluorescent hypoxia probe. *Int J Radiat Oncol Biol Phys* 22,
386 397–402. doi: 10.1016/0360-3016(92)90840-e.
- 387 Ong, S.-M., Zhao, Z., Arooz, T., Zhao, D., Zhang, S., Du, T., et al. (2010). Engineering a
388 scaffold-free 3D tumor model for in vitro drug penetration studies. *Biomaterials* 31,
389 1180–1190. doi: 10.1016/j.biomaterials.2009.10.049.
- 390 Pinho, D., Santos, D., Vila, A., and Carvalho, S. (2021). Establishment of Colorectal Cancer
391 Organoids in Microfluidic-Based System. *Micromachines (Basel)* 12, 497. doi:
392 10.3390/mi12050497.
- 393 Rohwer, N., and Cramer, T. (2011). Hypoxia-mediated drug resistance: novel insights on the
394 functional interaction of HIFs and cell death pathways. *Drug Resist Updat* 14, 191–
395 201. doi: 10.1016/j.drug.2011.03.001.
- 396 Thakuri, P. S., Gupta, M., Plaster, M., and Tavana, H. (2019). Quantitative Size-Based
397 Analysis of Tumor Spheroids and Responses to Therapeutics. *ASSAY and Drug*
398 *Development Technologies* 17, 140–149. doi: 10.1089/adt.2018.895.
- 399 Thippabhotla, S., Zhong, C., and He, M. (2019). 3D cell culture stimulates the secretion of in
400 vivo like extracellular vesicles. *Sci Rep* 9, 13012. doi: 10.1038/s41598-019-49671-3.
- 401 Weeber, F., van de Wetering, M., Hoogstraat, M., Dijkstra, K. K., Krijgsman, O., Kuilman,
402 T., et al. (2015). Preserved genetic diversity in organoids cultured from biopsies of
403 human colorectal cancer metastases. *Proc Natl Acad Sci U S A* 112, 13308–13311.
404 doi: 10.1073/pnas.1516689112.
- 405 Wisdom, K. M., Adebowale, K., Chang, J., Lee, J. Y., Nam, S., Desai, R., et al. (2018).
406 Matrix mechanical plasticity regulates cancer cell migration through confining
407 microenvironments. *Nat Commun* 9, 4144. doi: 10.1038/s41467-018-06641-z.
- 408 Zschenker, O., Streichert, T., Hehlhans, S., and Cordes, N. (2012). Genome-wide gene
409 expression analysis in cancer cells reveals 3D growth to affect ECM and processes
410 associated with cell adhesion but not DNA repair. *PLoS One* 7, e34279. doi:
411 10.1371/journal.pone.0034279.

413 **Figure 1. Morphological characterization of cancer cell lines cultured in LOT in flat-**
414 **bottom 96-well plates at day ten after seeding.** Lung adenocarcinoma (A549), prostate
415 adenocarcinoma (DU145, LnCaP, PC3), colorectal adenocarcinoma (Caco-2, HT29),
416 osteosarcoma (MNNG/HOS) and glioblastoma (U251) cell lines were grown for 10 days in
417 3D. Scale bar corresponds to 500 μm .

418

419 **Figure 2. Comparison of the culture plate impact on repeatability of the spheroids**
420 **formed with LOT.** A549 (A), LnCaP (B), MNNG/HOS (C) and U251 (D) cell lines were
421 seeded either in flat- or round-bottom 96-well plates and were cultured for up to 30 days using
422 LOT. Their morphology (diameter, roundness, number of spheroids) was measured with light
423 microscopy. Statistical test: Two-way Anova with the Geisser-Greenhouse's and Šídák's
424 corrections, $*p < 0.05$.

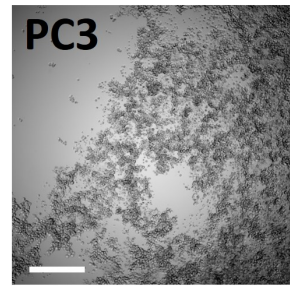
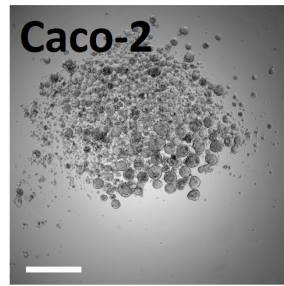
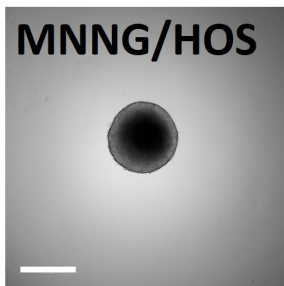
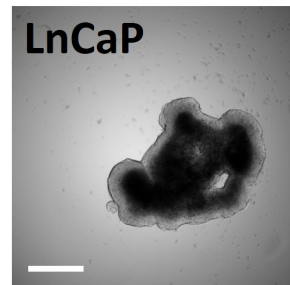
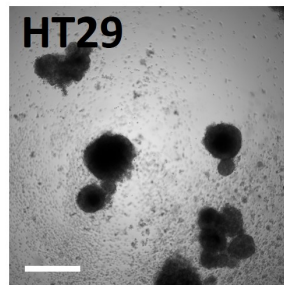
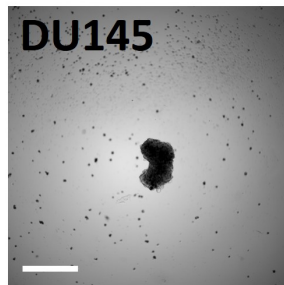
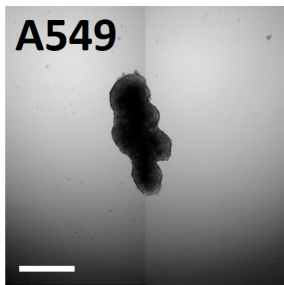
425

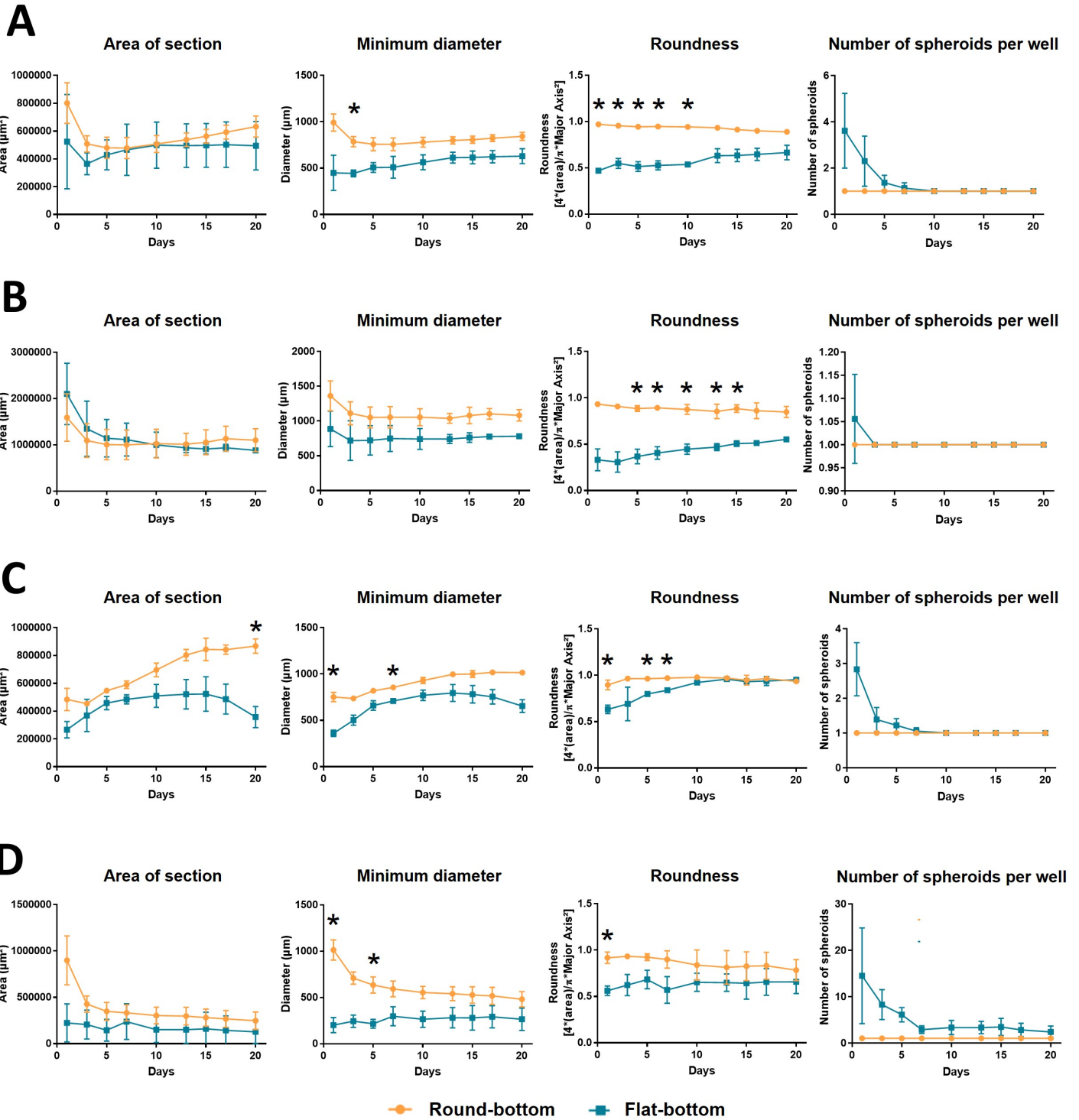
426 **Figure 3. Comparison of the culture volume or the culture method on the morphology of**
427 **spheroids 10 days after seeding.** The morphological characteristics of A549 (A), LnCaP (B),
428 MNNG/HOS (C) and U251 (D) seeded in round-bottom 96- or 384-well plates and grown
429 with LOT or seeded in round-bottom 96-well plates and grown with HD were measured with
430 light microscopy 10 day after seeding. Statistical test: Mann-Whitney two-sided, comparison
431 with LOT round-bottom condition; n.s., non-significant

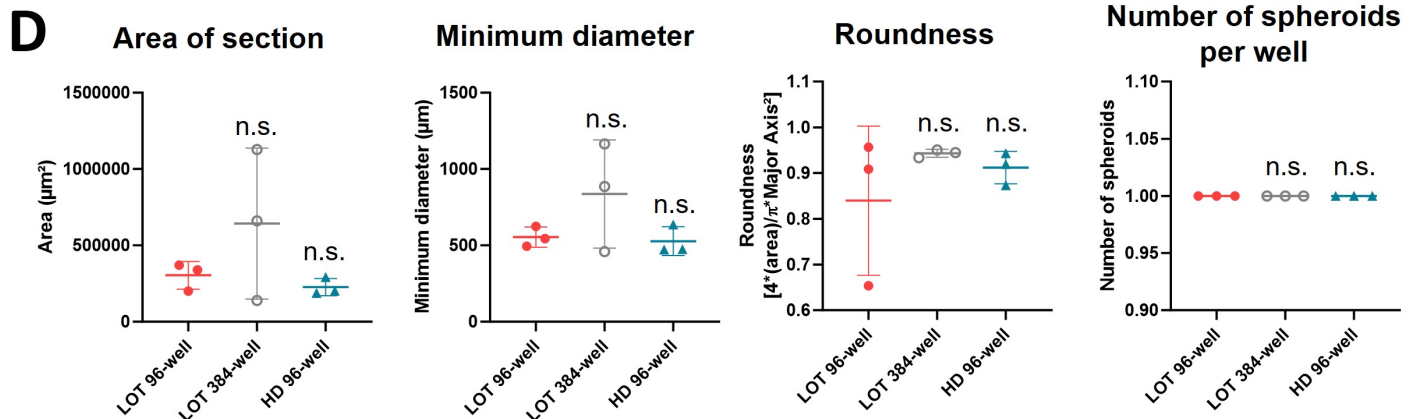
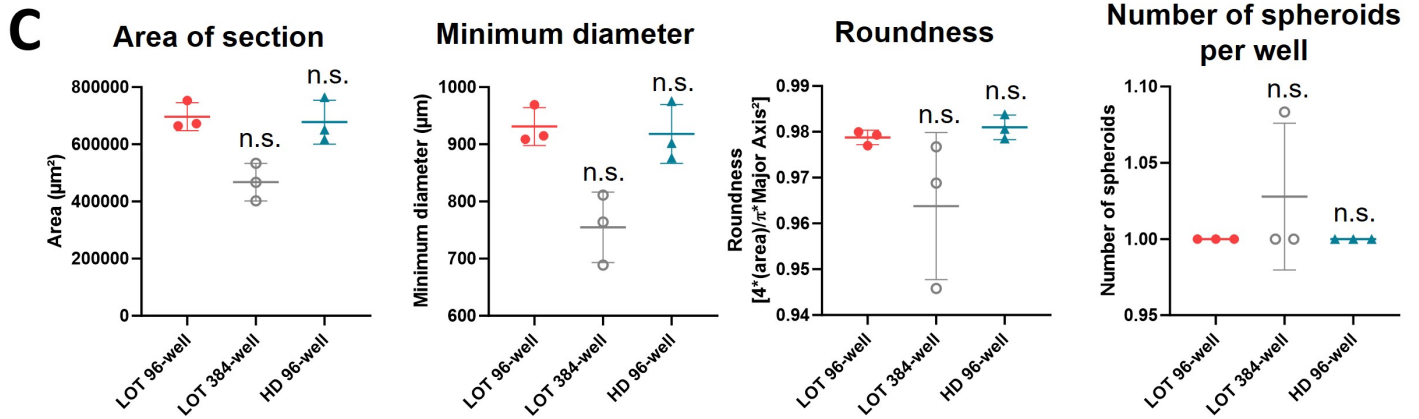
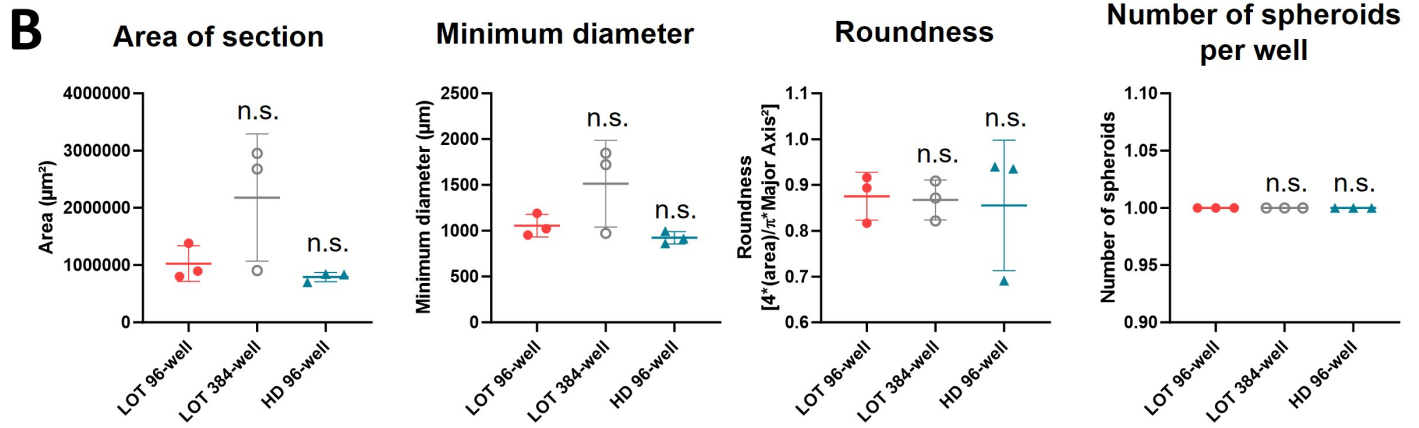
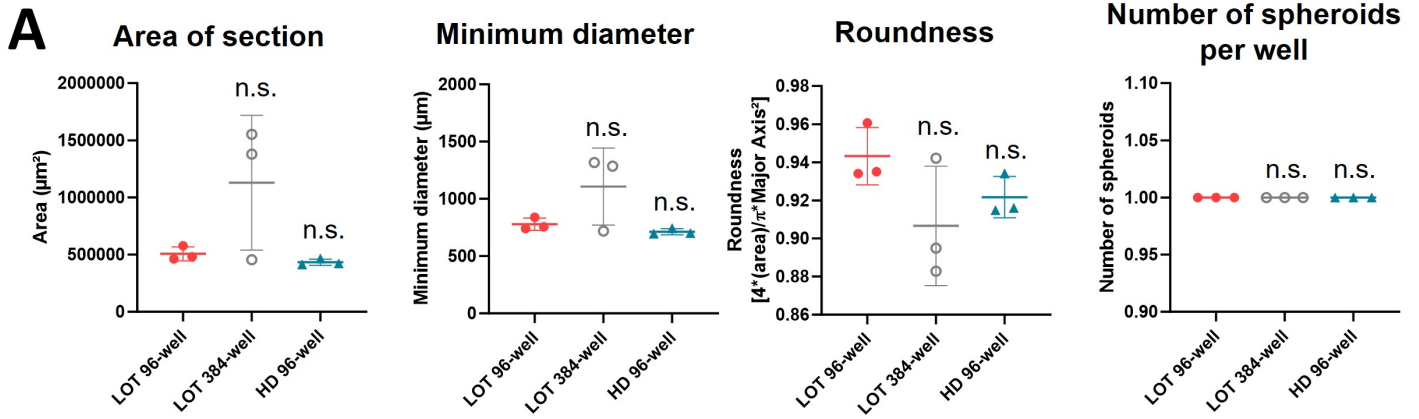
432

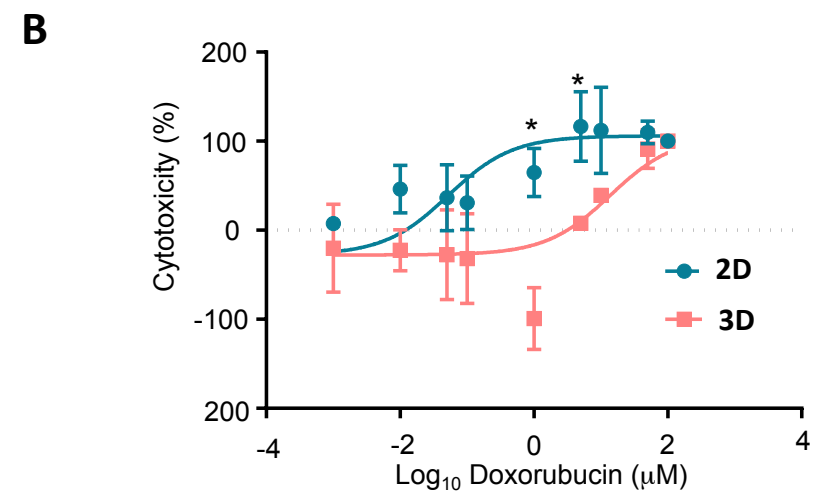
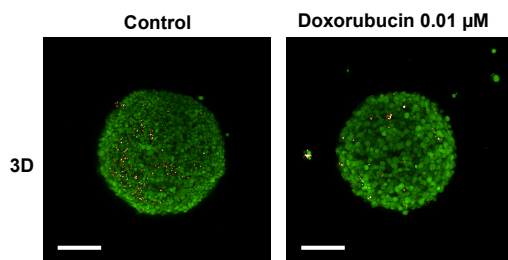
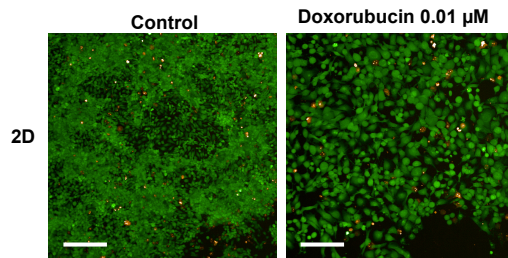
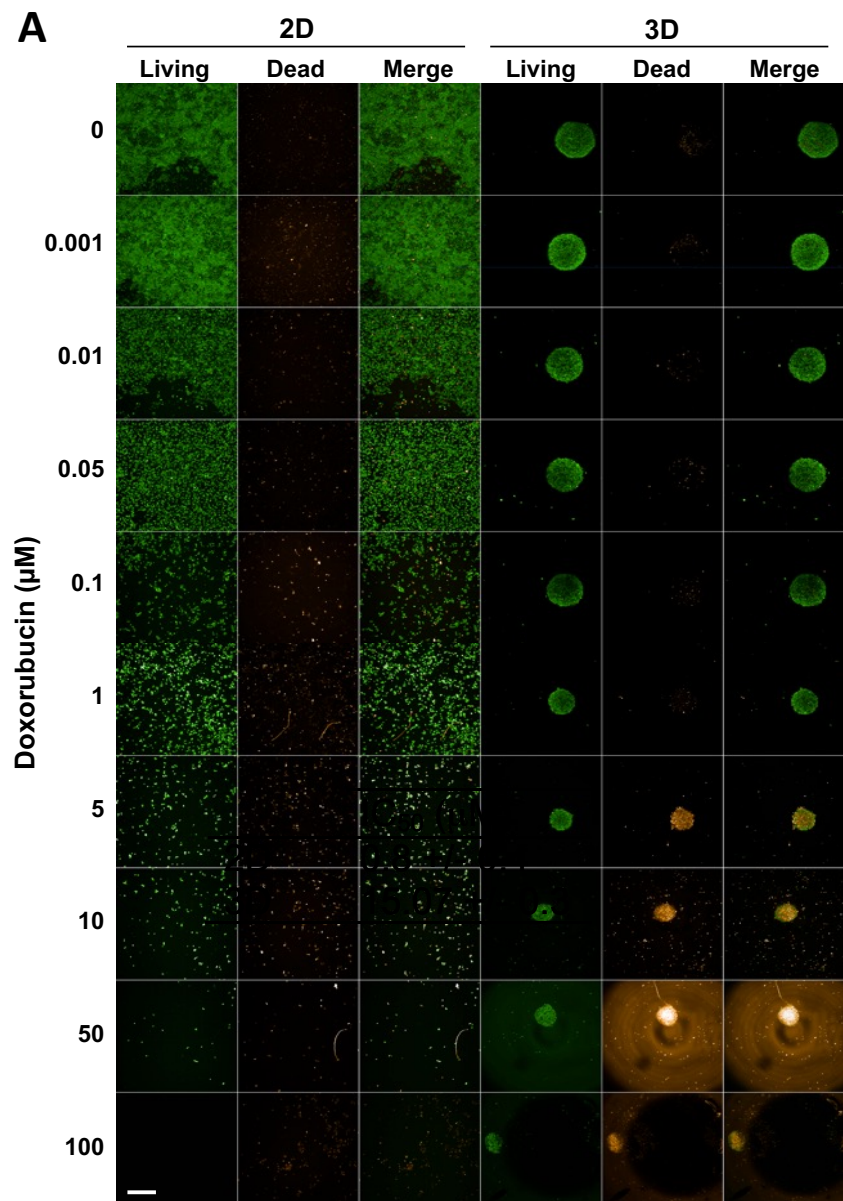
433 **Figure 4. Comparison of the sensitivity to chemotherapy treatment of MNNG/HOS cells**
434 **grown in 2D or 3D.** MNNG/HOS cells were cultured in 2D or 3D in adherent flat-bottom 96-
435 well plates and low-adherent round-bottom 96-well plates respectively. The cell monolayers
436 or spheroids were subjected to various doxorubicin concentrations over 72 hours. (A) The cell
437 cytotoxicity was measured with LIVE/DEADTM labelling. Green coloration corresponds to

438 live cells. Orange coloration corresponds to dead cells. Scale bar: 500 μm . (B) The dose-
439 response curves were obtained from the test results of the LDH release assay. Statistical test:
440 Two-way Anova with the Šídák's corrections, $*p < 0.05$.
441









	IC ₅₀ (μM)
2D	0.8 +/- 0.4
3D	15.07 +/- 0.3